

Precipitation in LiF Crystals Doped with MgF₂*

E. LILLEY†, J. B. NEWKIRK‡

Materials Science Center, Cornell University, Ithaca, NY, USA

Received 2 June 1967

X-ray, and optical and electron microscopy studies have been made of precipitation in single crystals of LiF doped with MgF₂. MgF₂ was found to nucleate only with difficulty, which probably accounts for the large MgF₂ precipitates that were observed. However, a metastable phase was discovered which readily nucleated, and, at low concentrations (e.g. 0.045 mol % MgF₂), it formed even on slow cooling. Its structure appears to be similar to that proposed by Suzuki for the NaCl/CdCl₂ system. The morphology of the metastable phase was seen by electron microscopy to be intersecting {100} platelets.

On holding crystals containing the metastable phase at temperatures of about 300° C, particles of MgF₂ nucleated at, and grew at, the expense of the metastable phase. The observation of precipitation of the metastable phase at low Mg⁺⁺ ion concentrations is notable, for precipitation has almost certainly occurred during other studies of ionic conductivity, dielectric loss, and colour centres, etc., where crystals have been held at temperatures below 250° C.

Solid-solubility measurements have been made to establish the MgF₂ solvus line at concentrations up to 6.5 mol % MgF₂ and the metastable phase solvus line up to 0.225 mol % MgF₂.

Kinetic measurements indicate that the growth of the metastable phase is controlled by bulk diffusion of Mg⁺⁺ ions, whereas the growth of MgF₂ appears to be controlled by the motion of vacancy pairs.

1. Introduction

Our knowledge of precipitation in ceramics when compared with metallic systems is limited and unsystematic. This is not surprising, for high-melting-point ceramic materials present serious experimental difficulties. The alkali halides, on the other hand, with their simple low-melting-point structures are much more attractive for a basic study of precipitation and should yield results relevant to the more complex ionic systems. Such a study would be able to draw on the vast body of research carried out on point and line defects in alkali halide crystals and also make a contribution to that research by indicating the influence of precipitation on several phenomena traditionally studied in

doped crystals (e.g. ionic conductivity, dielectric loss, and colour centres).

In the past, X-ray studies of precipitate structures have been made in the NaCl/CaCl₂ [1-4] and NaCl/CdCl₂ [5, 6] systems, but no attempt was made in these studies to investigate either the solubility at low doping concentrations, or the mechanisms of precipitation. These studies did reveal, however, that quenching and ageing of NaCl doped with CaCl₂ caused the precipitation of a metastable phase which is similar to the CaCl₂ structure. Similarly, a metastable phase was also found in the NaCl/CdCl₂ system and this was thought to have a stoichiometry of 6NaCl.CdCl₂.

Ionic conductivity has been used to study

*Part of a thesis presented for the degree of Doctor of Philosophy at Cornell University.

†Now at the School of Applied Sciences, University of Sussex, Brighton, UK.

‡Now Phillipson Professor, Metallurgy Department, University of Denver, Colorado, USA.

solubility of divalent ions in alkali halide crystals [7] at concentrations up to about 1.0 mol %. This method, used on its own, is limited, because it does not indicate what phase is precipitating, and, in particular, whether it is a stable or a metastable phase.

A study of LiF doped with MgF_2 was decided upon for the above general reasons and, in particular, because: (i) this system exhibits a high degree of solubility [8], so that it is possible to avoid eutectic transformations at concentrations of a few per cent MgF_2 (see fig. 1);

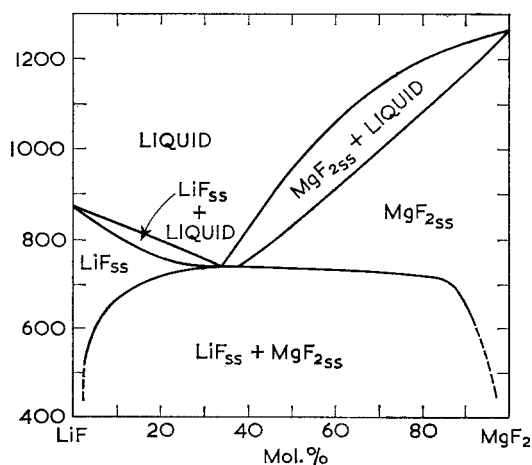


Figure 1 LiF/ MgF_2 phase diagram [8].

and (ii) LiF is quite transparent to X-rays, and thereby allows the study of low concentrations of the precipitated phase, within the LiF, by X-ray diffraction.

2. Techniques

LiF crystals doped with 0.045 and 0.225 mol % MgF_2 were grown by the Czochralski method; X-ray diffraction tests showed these to be homogeneous. Crystals containing up to 6.5 mol % MgF_2 were grown by the Bridgman method; these were shown to be somewhat segregated.

Optical microscopy was used to observe precipitates in LiF at low magnifications, and replica electron microscopy was used for the higher magnifications. Standard X-ray diffractometer and camera techniques were employed to study the structures and mechanisms of precipitation. A heater, shown in fig. 2, was applied, in conjunction with a single-crystal orienter, to study phase transformations by

*The Bragg angles of the precipitate spots were consistent with the normal MgF_2 (tetragonal rutile) structure.



Figure 2 Single-crystal heater for use on a diffractometer.

means of X-ray diffraction at elevated temperatures. This heater consists of a beryllium tube, heated by conduction from both ends, which transmits heat to the crystal inside and is transparent to X-rays. It is capable of operation at temperatures from room temperature up to 630°C to an accuracy of $\pm 1^\circ\text{C}$. A small crystal placed inside the heater can be oriented at positions where the precipitate particles diffract the strong characteristic X-rays. The area under the resultant Bragg peak gives a proportionate measure of the volume of precipitate present. The low heat capacity of the heater allows the temperature to be raised or lowered moderately quickly (e.g. at a rate of about $20^\circ\text{C}/\text{min}$ at the temperatures of interest).

3. Precipitation of MgF_2

Rotating crystal photographs, made of very slowly cooled LiF single crystals containing 1.8 mol % MgF_2 , revealed not only LiF layer-line reflections, but also reflections from MgF_2 precipitate particles.* The authors have pre-

viously published such photographs and, using the data contained therein, have deduced the orientation relation between the LiF matrix and the MgF₂ precipitate particles [9]. The relationship is

$$\begin{matrix} \{111\}_{\text{LiF}} & || & \{100\}_{\text{MgF}_2} \\ \langle 0\bar{1}1 \rangle_{\text{LiF}} & || & \langle 011 \rangle_{\text{MgF}_2} \end{matrix}$$

There are twenty-four orientation variants within this definition.

Cylindrical Laue photographs of the same crystals exhibited some unusual diffraction features. These consisted of streaks and crosses, the most striking of which was a double cross centred on the transmission hole when the X-ray beam was normal to the {100}_{LiF} planes (fig. 3). The ends of each streak were more intense than the middle. Because the crystals had been slowly cooled and contained large precipitates, the streaks could not have been caused by Guinier-Preston zones. When the cross was plotted in stereographic projection, both ends of each segment of the cross were found to correspond

to two of the {111}_{MgF₂} reflections which arise from the twenty-four possible orientations of the precipitate particles. The streaks did not correspond to any crystallographic direction but rather were the result of deviations from the specified orientation relation. The twenty-four possible orientation variants can be divided into twelve pairs, each of which have mutually parallel (100)_{MgF₂} planes and [011]_{MgF₂} vectors inclined at 7° to each other. The stereographic plot reveals that the streaks are due to some of the MgF₂ particles being oriented with their [011] vectors somewhere within this 7° range, but still having their {100}_{MgF₂} || {111}_{LiF}. However, the majority of the particles were oriented close to the ideal relationship.

3.1. Morphology of MgF₂ Precipitates

Single crystals of LiF grown by the Bridgman technique containing 1.8 mol % MgF₂ were cloudy owing to precipitation. The transparency of the LiF allows the microscope to be focused inside the crystal on the MgF₂ particles, which

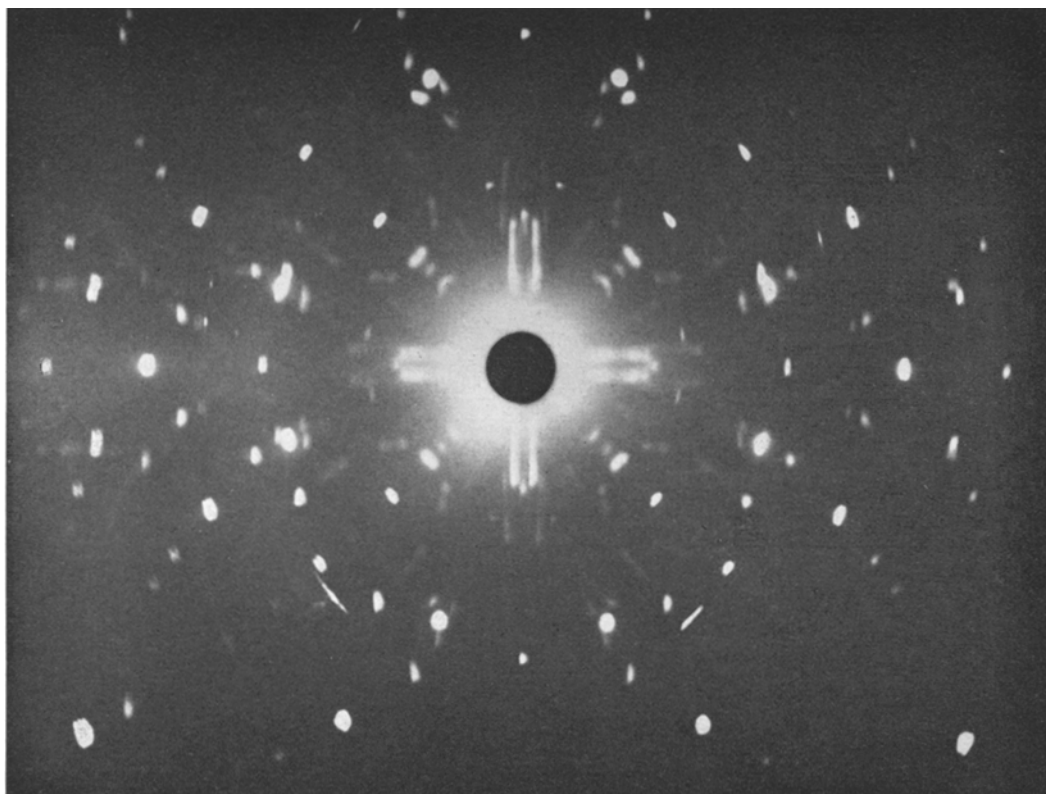


Figure 3 A {100}_{LiF} oriented transmission cylindrical Laue photograph of a slowly cooled 1.8 mol % MgF₂ crystal. The LiF crystal has a <100> axis parallel to the film. The crosses and streaks are associated with the MgF₂ precipitates.

appear white when viewed between crossed polarisers. At low magnifications, the precipitates are seen as intersecting rods lying in regular directions and forming planes in the crystal. Fig. 4 shows some but not all of the MgF_2 rods

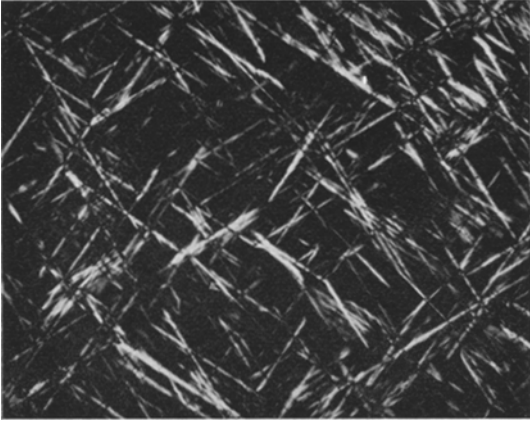


Figure 4 Network of MgF_2 precipitates lying in planes close to $\{111\}_{\text{LiF}}$, seen inside a LiF single crystal – polarised light – 1.8 mol % MgF_2 ($\times 25$).

which formed inside the crystal. Other rods are invisible because they are in an extinction position. Angular measurements of the rods relative to the LiF cube edges, made with a universal stage, indicate that the intersecting rods lie in planes close to, but not coincident with $\{111\}_{\text{LiF}}$. The poles of these planes make an angle with the $[001]_{\text{LiF}}$ axis, which varies slightly about a mean of 60° as opposed to $54^\circ 44'$ made by a $(111)_{\text{LiF}}$ pole. Pairs of rods are symmetrical about the $[110]_{\text{LiF}}$ vector included in the plane, and each is inclined at about 22° to this vector. The directions of the individual rods, although regular, do not correspond to any rational low index directions. Nor is there any obvious correspondence between the direction of the rods and the “grown-in” dislocations as revealed by our ultramicroscopic observations and those of Washburn and Nadeau [10].

At higher magnifications, the MgF_2 precipitates are seen to be blade-like with saw-tooth edges rather than simple rods. Part of a particularly large particle, shown in fig. 5, had been extracted from the matrix by dissolving the latter

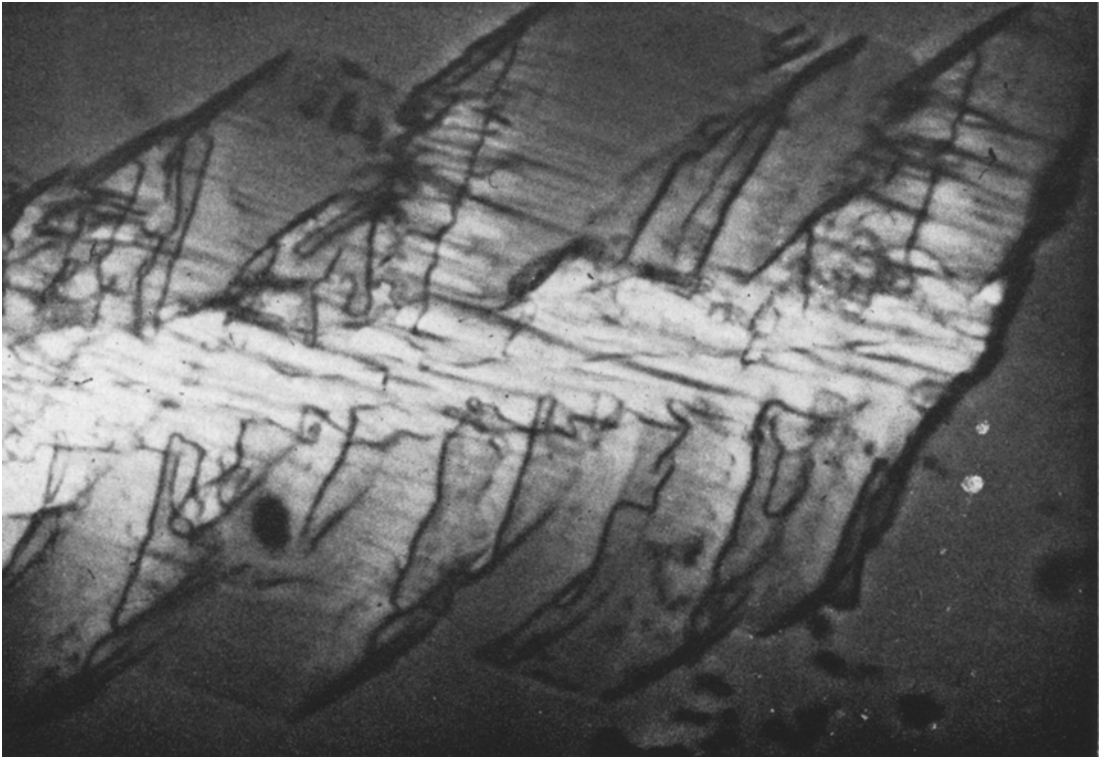


Figure 5 An unusually large MgF_2 particle which has been extracted from the LiF matrix – transmitted light ($\times 430$).

in a dilute ammonia solution. The edges of the particle correspond to alternate $[001]_{\text{MgF}_2}$ and $[011]_{\text{MgF}_2}$ directions. (This was deduced by observing the extinction direction of the precipitate and confirmed by relating these edges to the LiF axes, making use of the known orientation relationship.)

The broad surfaces of the MgF₂ particles appear to be $\{100\}_{\text{MgF}_2}$ faces, stepped along their length. It is possible that the growth of the precipitates took place in a stepwise process and that the final particles are a combination of a series of individual units. This would account for the individual units having $\{100\}_{\text{MgF}_2}/\{111\}_{\text{LiF}}$ interfaces and yet allow the blades as a whole to be non-parallel to the $\{111\}_{\text{LiF}}$ planes.

It was also found that the precipitate morphology was independent of cooling rate, for, even in crystals which had been cooled quickly enough to allow only small (5 μm wide) MgF₂ particles to grow, the same morphology resulted. This observation was made on extracted precipitate particles using electron microscopy.

4. Precipitation of the Metastable Phase

In the last section, it was shown that MgF₂ having its normal equilibrium structure would precipitate from slowly cooled, heavily doped LiF crystals. However, rapid cooling by air blasting, or quenching into silicone oil caused a metastable phase to precipitate instead of the MgF₂. This same phase was also formed in slowly cooled crystals containing 0.045 and 0.225 mol % MgF₂.

4.1. X-ray Analysis

Fig. 6 shows an X-ray rotation photograph of a quenched 1.8 mol % MgF₂ crystal. The metastable phase has resulted in extra layer lines of reflections on the photograph. Metastable precipitate reflections appear both midway between the LiF layer lines, and nearly coincident with the LiF reflections. The diffraction spots of the metastable phase are not as strong as those of the LiF and are more diffuse. An analysis of the diffraction pattern revealed that the metastable phase is cubic, with a cell size of 8.20 Å, slightly more than double that of LiF.

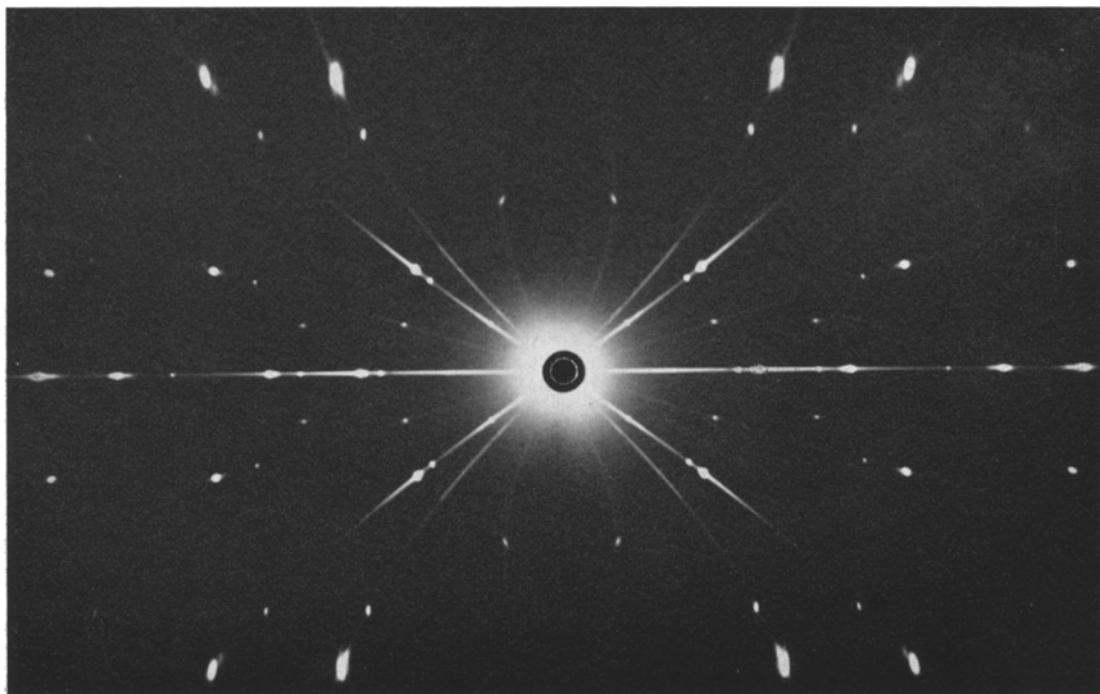


Figure 6 Single-crystal rotation photograph of a rapidly cooled crystal containing 1.8 mol % MgF₂. The strong layer-line reflections are due to $K\alpha$ and $K\beta$ reflections of LiF and the weaker ($K\alpha$) layer lines to a metastable precipitate phase. (The $K\beta$ reflections from this phase are too weak to see on the print.) Unfiltered Cu radiation, and a $\langle 100 \rangle_{\text{LiF}}$ rotation axis were used.

Its cube axes were parallel to those of the LiF matrix. The structure appeared at first sight to be analogous to that found by Suzuki in the system NaCl/CdCl₂ [5], shown in fig. 7. Suzuki's

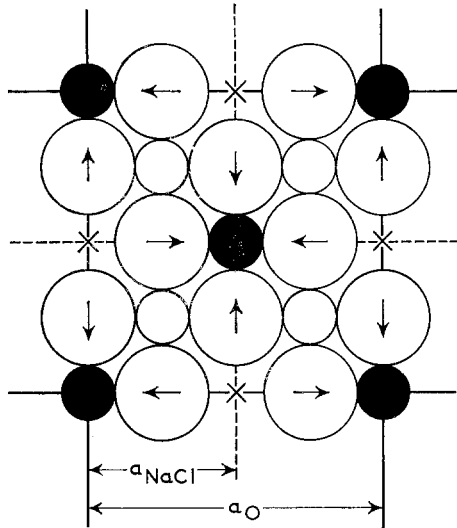


Figure 7 Arrangement of ions in the (100) plane of the proposed cell of 6NaCl.CdCl₂. Small, solid circles represent Cd⁺⁺ ions; small, open circles - Na⁺ ions; large, open circles - Cl⁻ ions; and crosses - cation vacancies. Arrows indicate the displacement of Cl⁻ ions (After Suzuki [5].)

model is essentially an ordered arrangement, on the NaCl lattice, of the Na⁺ and Cd⁺⁺ ions, cation vacancies, and Cl⁻ ions, the latter retaining their original sites but being displaced slightly as shown. The structure was verified by Tolman [6], who calculated that the displacement of the Cl⁻ ions was 0.014a₀. The structure proposed by Suzuki has the stoichiometry 6NaCl.CdCl₂.

In an endeavour to analyse the structure of the metastable precipitate phase in the LiF/MgF₂ system, intensity measurements of a series of reflections were made on a diffractometer, using a LiF single crystal containing the metastable precipitate particles. The measurements were difficult to make because of the low concentration and fine dispersion of the precipitates in the crystal and they were probably not very accurate. Consistent with the observations of Suzuki, it was found that the (333) and (731) metastable-phase reflections are missing, and that the intensities for (331), (600), (711), and (771) reflections are very low. Suzuki's

model was used in an attempt to explain the observed intensities, trying various values for the displacement of the anions, δ . With no displacement ($\delta = 0$), very poor agreement was found between the measured and calculated intensities. (Relative intensities rather than absolute intensities were used, so that it was necessary to make comparisons for a series of reflections.) The best agreement was found using $\delta = 0.010a_0$, though this still gave poor agreement for (200) and (220) reflections. This discrepancy, however, was reduced if some of the Mg⁺⁺ ions were randomised on the cation lattice from the positions of Suzuki's model. After performing calculations for various modes of randomising, we concluded that the best modification of the Suzuki model is one in which two of the four Mg⁺⁺ ions are on sites as proposed by Suzuki, with the other two randomly dispersed on the Li⁺ ion sites; correspondingly, two Li⁺ ions per unit cell are randomly arranged on the Mg⁺⁺ ion lattice. The F⁻ ions are displaced 0.010a₀ from their normal positions, approximately as shown in fig. 7.

4.2. Morphology of the Metastable Precipitates

In order to study the morphology of the metastable phase, replicas were made of a crystal of LiF/0.225 mol % MgF₂, which had been slowly cooled and was known, from X-ray diffraction observations, to contain the metastable phase but no stable MgF₂. The replicas were made by shadowing platinum and graphite onto a freshly cleaved surface of the crystal. After the replica had been divided into 2 mm squares by scribing the surface, the crystal was immersed in a dilute solution of ammonia which dissolved the LiF. The replicas floated off and were collected on grids for examination in the electron microscope. Fig. 8 shows a replica of the metastable precipitate particles which appear as crosses. By using shadowing in a <100> direction as a crystallographic marker, it was found that the arms of the crosses lay in those same directions. It is clear that the metastable precipitates are composed of intersecting {100} platelets which have dimensions approximately 0.3 μm long parallel to <001> and 0.05 μm wide.

The volume fraction of the precipitates shown in fig. 8 is about 2%. This is in agreement with that calculated for a concentration of LiF/0.225 mol % MgF₂, assuming the structure

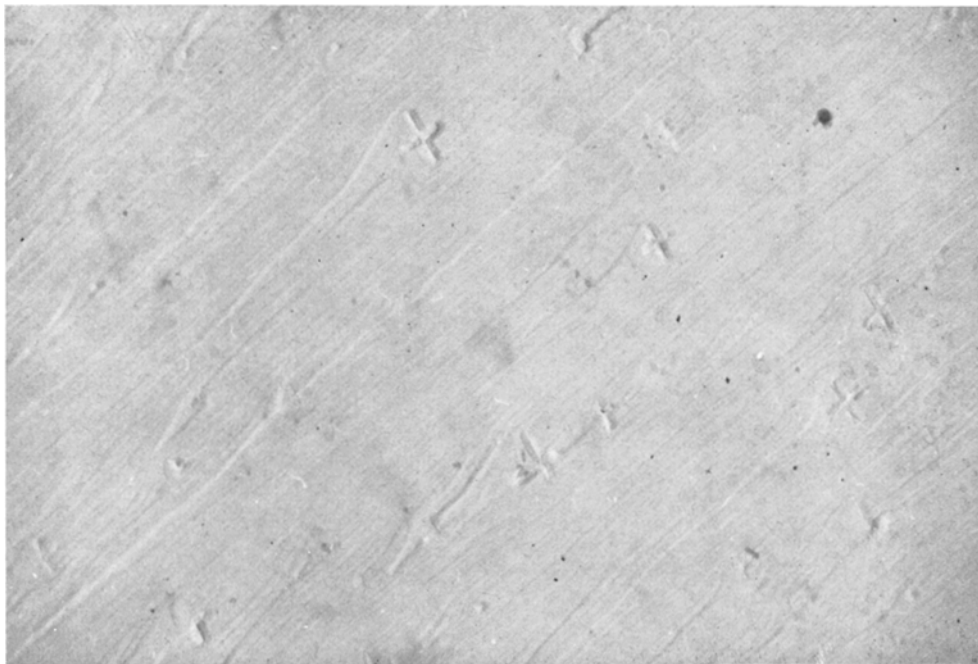


Figure 8 Metastable precipitate particles which have formed as intersecting $\{100\}_{\text{LiF}}$ platelets in the LiF matrix – replication of $\{100\}_{\text{LiF}}$ surface of a slowly cooled 0.225 mol % MgF₂ crystal ($\times 30\,000$).

proposed by Suzuki, and on the basis of a 6LiF.MgF₂ stoichiometry.

5. Mechanisms of Precipitation

In the previous sections, the structure and morphology of the stable and metastable precipitates and their crystallographic relationship to the LiF matrix were discussed. Now the effect of temperature, composition, and cooling rate on the formation and stability of the two phases will be considered.

Specimens from the LiF/1.8 mol % MgF₂ crystal were cooled at different rates from about 600° C and were examined by X-ray diffractometry. Very slow cooling caused the formation of the stable MgF₂ phase. Air blast cooling of small crystals caused the formation of the metastable phase previously described. With decreasing MgF₂ concentration, it became increasingly difficult to form the stable MgF₂ phase even with very slow cooling. For example, furnace-cooling at about 100° C/h of a 0.045 mol % MgF₂ crystal caused the formation of the metastable phase.

The results of the continuous cooling experiments are somewhat misleading, for it was found that the metastable phase could transform to MgF₂ at about 300° C. The following

observations show that MgF₂ formed at the expense of the metastable precipitate particles. A rapidly cooled LiF/1.8 mol % MgF₂ crystal was mounted in the heater (fig. 2). The X-ray intensity diffracted by the (113) planes of the metastable phase was measured, first at 300° C and then at 330° C, as a function of time. An identical crystal was then oriented in the heater to diffract the (110) reflections of the stable MgF₂ phase which was initially absent in the rapidly cooled crystal. By holding the crystal at 300 and 330° C for the same times as for the first crystal, and observing the diffracted intensity, the formation and growth of the MgF₂ was observed. The results shown in fig. 9 indicate that there is a definite correspondence between the formation of the stable phase and the disappearance of the metastable phase.

Replicas of freshly cleaved crystals, examined in the electron microscope, showed MgF₂ precipitate particles which frequently occurred as pairs or clusters (fig. 10). These pairs or clusters have about the same mean separation as the metastable precipitates shown in fig. 8. As would be expected, they are considerably smaller in size than the crosses, since the metastable phase contains only 14 mol % MgF₂. It appears that each metastable precipitate has

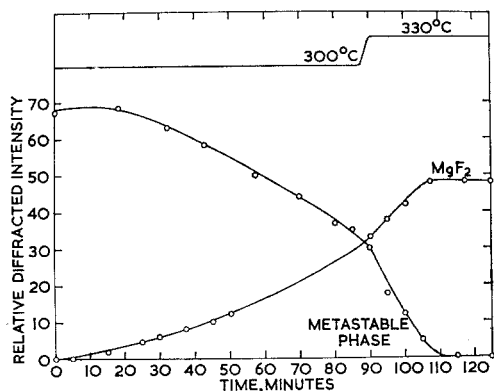


Figure 9 Plot of the relative X-ray intensities diffracted by both the metastable and MgF_2 precipitates as a function of time at 300 and 330°C. The growth of the MgF_2 phase is taking place at the expense of the metastable phase.



Figure 10 Replication electron micrograph of 0.225 mol % MgF_2 crystal in which the metastable precipitates had previously transformed to MgF_2 ($\times 43\,680$). The MgF_2 precipitates have a shape different from the metastable crosses of fig. 8.

nucleated several MgF_2 particles, probably on the original precipitate surface. If this is the case, the transformation cannot be one involving a local rearrangement of atoms within the metastable particles, for they contain a high concentration of Li^+ ions which must be rejected in the formation of the stable MgF_2 . Thus the growth of MgF_2 will involve bulk diffusion of Li^+ and Mg^{++} ions.

In the X-ray study of the formation of MgF_2 from the metastable phase, it was found that the temperature at which the transformation began

*In spite of the fact that the diagram, as taken from reference 8, shows a solid curve down to about 2 mol % MgF_2 .

depended on the prior heat-treatment of the crystal. Crystals of $\text{LiF}/0.225$ mol % MgF_2 which had been slowly cooled, and therefore presumably contained relatively large metastable precipitate particles, transformed at about 260°C during the elevated temperature examination. Quickly cooled crystals containing finer precipitate particles, as evidenced by broad X-ray diffraction peaks, would not transform until about 300°C. With lower concentrations (e.g. 0.045 mol % MgF_2), it is difficult to induce the transformation, for it is necessary to hold the crystals below the solvus temperature, 295°C for that composition. (The solvus lines for the metastable phase and the MgF_2 , at low concentrations, are shown in fig. 11. The determination of these lines is described in the next section.)

An unusual way was found to enhance the nucleation of MgF_2 . This was to irradiate with X-rays a crystal containing metastable precipitate particles, prior to heat-treatment. The MgF_2 then formed at a lower temperature than in an unirradiated crystal (e.g. for $\text{LiF}/0.225$ mol % MgF_2 , at a temperature of about 290°C in an irradiated crystal and about 330°C in an unirradiated crystal).

In addition to qualitative studies of the ease of nucleation of MgF_2 , measurements were made of the degree of undercooling necessary for the precipitation of MgF_2 from solid solution. With a crystal containing 0.225 mol % MgF_2 , it was found that the MgF_2 first formed at about 355°C after cooling from 500°C. By referring to the solvus lines in fig. 11, it may be seen that about 100°C undercooling is necessary for nucleation at this concentration. However, it should be noted that 355°C is below the metastable-phase solubility line (which is not very accurate in this region). It is therefore quite possible that the MgF_2 did not nucleate directly from solid solution, but sequentially, after the precipitation of the metastable phase.

6. Solubility of MgF_2 and the Metastable Phase in LiF

The LiF/MgF_2 phase diagram shown in fig. 1 contains no datum points below 10 mol % MgF_2 .* It is possible, however, using the disappearing-phase technique [11], to measure the solid solubility at lower concentrations with fair accuracy. This method involves using X-ray diffraction to find the minimum temperature at

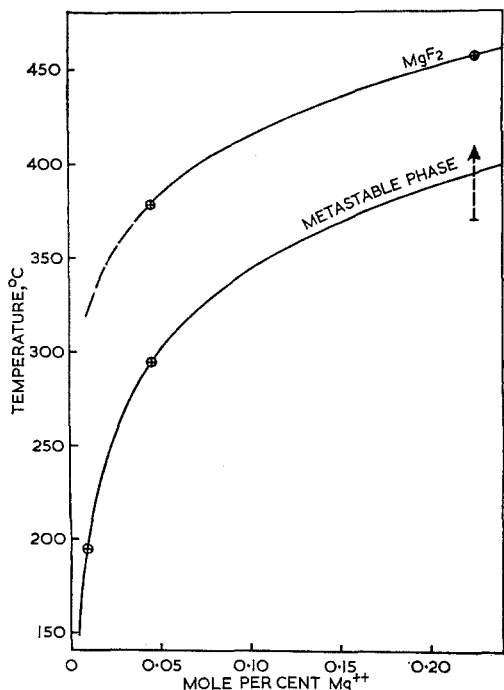


Figure 11 Part of the LiF/MgF₂ phase diagram showing the metastable and stable MgF₂ solvus lines up to 0.25 mol % MgF₂. The upper solvus line represents equilibrium between MgF₂ and the homogeneous solid solution.

which the precipitate phase completely dissolves. By using single-crystal specimens and employing the heater shown in fig. 2 on an X-ray diffractometer, it was possible to obtain measurable Bragg peaks from precipitate particles at concentrations of 0.045 mol % MgF₂ in LiF. The {110} planes of MgF₂ and the {311} planes of the metastable phase were selected for diffraction because these planes gave a high, relative, diffracted intensity. By appropriate heat-treatment, it was possible to obtain either stable MgF₂ or else the metastable phase in the absence of the other phase. The results are recorded in fig. 11.

Some difficulty was encountered in determining the solvus line of the metastable phase at temperatures above 300° C because the metastable phase transformed to the equilibrium MgF₂ structure. The 0.225 mol % MgF₂ datum point in fig. 11 was determined approximately by solution-treating the crystal at 500° C, lowering the temperature to about 300° C so that precipitation of the metastable phase just began, and then raising the temperature to locate the maximum temperature at which the precipitate would show some growth before the trans-

formation to MgF₂ set in. This temperature was then taken as the lower limit of the solvus temperature for the LiF/0.225 % MgF₂ crystal.

The lowest concentration datum point was obtained by holding a slowly cooled crystal containing 0.011 mol % MgF₂ at a series of temperatures for 4 h, followed by hardness measurements to find the discontinuity at which the precipitates dissolved. A solvus temperature of 195° C was found, which is a little lower than that found by Johnston [12] for the same crystal.

The solubility data derived from X-ray measurements are given in table I. The solvus lines of the metastable and the MgF₂ phases at compositions up to 0.25 mol % MgF₂ are shown in fig. 11, and the MgF₂ solvus line for compositions up to 7.0 mol % is shown in fig. 12.

TABLE I

Solubility of Mg ⁺⁺ as a mole fraction	Metastable phase solvus temperature (° C)	MgF ₂ solvus temperature (° C)
$(4.5 \pm 0.5) \times 10^{-4}$	295	378
$(2.25 \pm 0.25) \times 10^{-3}$	370	457
1.8×10^{-2}	—	560
6.5×10^{-2}	—	630

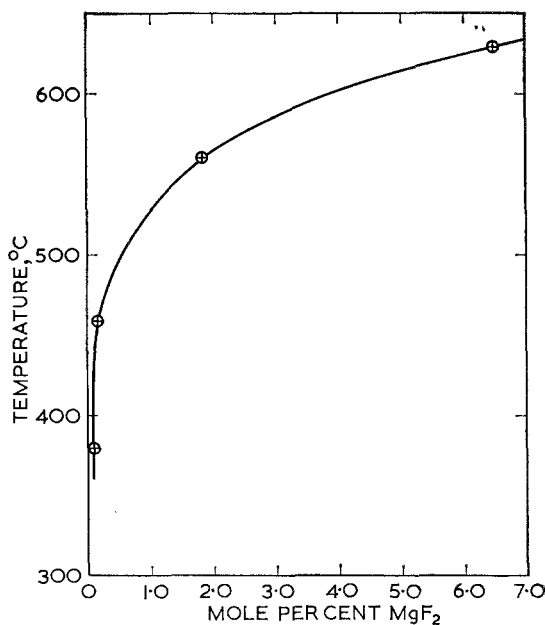


Figure 12 LiF/MgF₂ solvus line, 0 to 7.0 mol % MgF₂.

7. Kinetics of Precipitation

Qualitative observations regarding the formation of the MgF_2 and metastable precipitates have already been given, but little distinction was made between the processes of nucleation and growth. It was evident, however, that the nucleation rate of MgF_2 was low. Invariably, with step-wise heating, it was found that solution, or precipitation, occurred more rapidly for the metastable phase than for the MgF_2 . This is shown by the fact that the metastable particles came to equilibrium faster with the solid solution, at a given temperature, than did the MgF_2 particles, which had the same degree of dispersion in the crystal.

In order to obtain quantitative data for the rates of precipitation, measurements of X-ray intensities diffracted by precipitate particles were made as a function of time at elevated temperatures. The integrated intensity is proportional to the volume of precipitate present, where, as in this case, the temperature factor, the primary and secondary extinction, and absorption by the matrix are not important. These measured intensities were used in the change-of-slope method [13] to determine an activation energy for the process. In this method, the volume of precipitate present is measured as a function of time at a particular temperature T_1 , then the temperature is changed quickly and the measurements continued at a second temperature T_2 . In a plot of the volume precipitated versus time of precipitation, the two limiting slopes R_1 and R_2 , taken at the point of temperature change, are used in the following equation [13]

$$\log_e \left(\frac{R_1}{R_2} \right) = -(E/k) (1/T_1 - 1/T_2) \quad (1)$$

to obtain the activation energy E . k is the Boltzmann constant and temperature T_1 and T_2 are measured in degrees Kelvin.

7.1. Kinetics of Precipitation of MgF_2

Elevated-temperature X-ray diffraction measurements were made using the beryllium heater, so that the transformation process could be followed continuously as a function of time. To prevent nucleation during the measurements of the growth of MgF_2 , the following procedure was used. A crystal of 1.8 mol % MgF_2 was chosen which had previously been rapidly cooled from the solution range so that some of the Mg^{++} ions had precipitated as the metastable

phase but none as MgF_2 . Holding this crystal in the heater at 300°C caused the metastable precipitates to nucleate MgF_2 . The crystal was still, however, supersaturated with Mg^{++} ions, so that growth could take place at a reasonable rate and presumably without further nucleation. The growth of the MgF_2 was followed continuously, first at 395°C and then again after quickly raising the temperature to 445°C . The record of diffracted X-ray intensity as a function of time for the two temperatures is shown in fig. 13. The results are as follows: at $T_1 = 668^\circ\text{K}$, $R_1 = 1.68$; at $T_2 = 718^\circ\text{K}$, $R_2 = 0.16$.

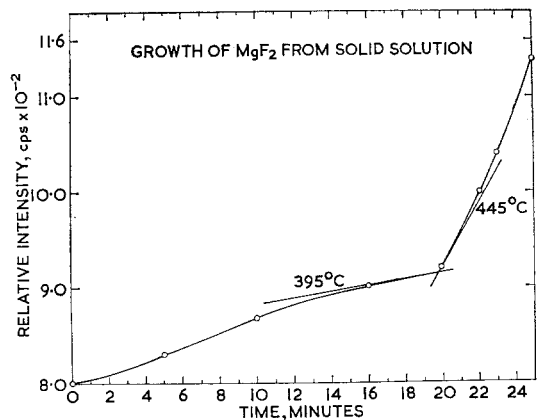


Figure 13 Kinetic data for the growth of MgF_2 from solid solution. The relative diffracted intensity in counts per second, which is proportional to the volume of precipitate present, is plotted as a function of time at 395 and 445°C .

Substitution of these values in equation 1 gave an activation energy, for growth of MgF_2 from solid solution, of 1.9 ± 0.1 eV. The same activation energy was found for the growth of the MgF_2 at the expense of the metastable phase.

7.2. Kinetics of Precipitation of the Metastable Phase

To avoid nucleation during growth measurements of the metastable phase, a slightly different approach was used. Crystals containing 0.225 mol % MgF_2 were cooled within the heater from the solution range to about 150°C to cause nucleation of the metastable phase. Then the temperature was raised to about 300°C , at which the growth rate was studied as described before. The changes in slope were much smaller than for the growth of MgF_2 , making the measurements much less accurate. An

average value, for the activation energy for growth of the metastable phase, of 0.75 ± 0.25 eV was found.

8. Discussion

8.1. Nucleation

The most striking difference between the two precipitates was that the equilibrium MgF₂ particles were large in size, whereas the metastable particles were small, even when formed by slow cooling. The main reason for this appears to be that the MgF₂ nucleates only with difficulty. The experiments carried out on solution-treated crystals containing 0.225 mol % MgF₂, to find the minimum temperature at which MgF₂ could be formed, indicated a temperature just below the metastable solvus line. This suggests that the MgF₂ may have formed via nucleation on the metastable phase rather than directly from solid solution.

Studies of the formation of MgF₂ from the metastable phase showed that the required temperature depended on the prior heat-treatment. The faster the crystals had been cooled, the higher the temperature necessary for the transformation. This may simply be due to a greater density of interface dislocations in the larger precipitate particles formed by slower cooling, which would assist the nucleation of MgF₂. Similarly, X-irradiation could generate colour centres in the metastable precipitate particles or in the matrix; colour centres cause lattice dilation and may thereby generate misfit dislocations at the precipitate/matrix interface.

It is expected that the barrier to nucleation of MgF₂ would be greater than that for the metastable phase, since an MgF₂ nucleus would involve atom displacements from both anion and cation matrix lattices, whereas a nucleus of the metastable phase would only involve a rearrangement of the Li⁺ and Mg⁺⁺ ions, and the extrinsic vacancies on the cation lattice. Nucleation of MgF₂ at the metastable precipitate particles rather than direct from solid solution is also aided by the higher concentration of the Mg⁺⁺ ions present in the metastable phase (14%), which increases the probability of nucleation [14]. A point about nucleation which will be amplified in the discussion of kinetics is that no substantial barrier to diffusion is anticipated at the nucleus/matrix interface of the metastable structure, whereas in the formation of a nucleus with an MgF₂ structure the F⁻ ions presumably must jump across the

interface. This may be a slow process.

Fig. 14 shows a hard-sphere model of F⁻ ions at the precipitate/matrix interface, which can be used as follows to understand how a range of precipitate orientations can occur in the {111}_{LiF} plane, in addition to those given by the previously stated orientation relation. The line-up of ions along the [0 $\bar{1}$ 1]_{LiF} direction corresponds to one of the twenty-four members of the orientation relation family. If the MgF₂ lattice is imagined to be rotated anticlockwise through 7°, the ions then line up along the [$\bar{1}$ 10]_{LiF} direction, giving another member of the orientation family. Orientations in-between these two positions still give good matching, which is probably the reason for the range of precipitate orientations implied by the X-ray diffraction pattern of fig. 3.

8.2. Precipitate Structures

Precipitation of a phase containing divalent ions from an alkali halide solid solution can take several different structural forms. The commonest of AB₂ type structures are tetragonal rutile (which is the structure of MgF₂), cubic fluorite, and orthorhombic CdCl₂. It is usually found that divalent halides have the rutile structure when the cations are small and the calcium fluoride structure when the cations are large [15].

Because there are nucleation difficulties associated with the precipitation of the stable phases, alkali halide crystals containing divalent impurities seem to be prone to the formation of metastable phases. Not only must the structure of the metastable phase resemble that of the matrix to nucleate easily, it must also maintain electrical charge neutrality. It is therefore necessary to incorporate in the metastable structure, with each divalent ion, an extrinsic vacancy. Suzuki proposed the model shown in fig. 7 which does this successfully for a NaCl type of structure. This model appears to account for the metastable phases formed in the NaCl/CdCl₂ and LiF/MgF₂ systems. In the latter case, X-ray measurements suggest that two of the four Mg⁺⁺ ions should be randomly mixed with the Li⁺ ions. The displacement of the anions, $\delta = 0.010a_0$, is similar to the value of $0.014a_0$ found by Tolman for the NaCl/CdCl₂ case. The lattice parameter of the LiF/MgF₂ metastable phase is 1.8% larger than the double cell of LiF, compared with the NaCl/CdCl₂ metastable phase which is only 0.3% larger than the double cell of NaCl. This is somewhat

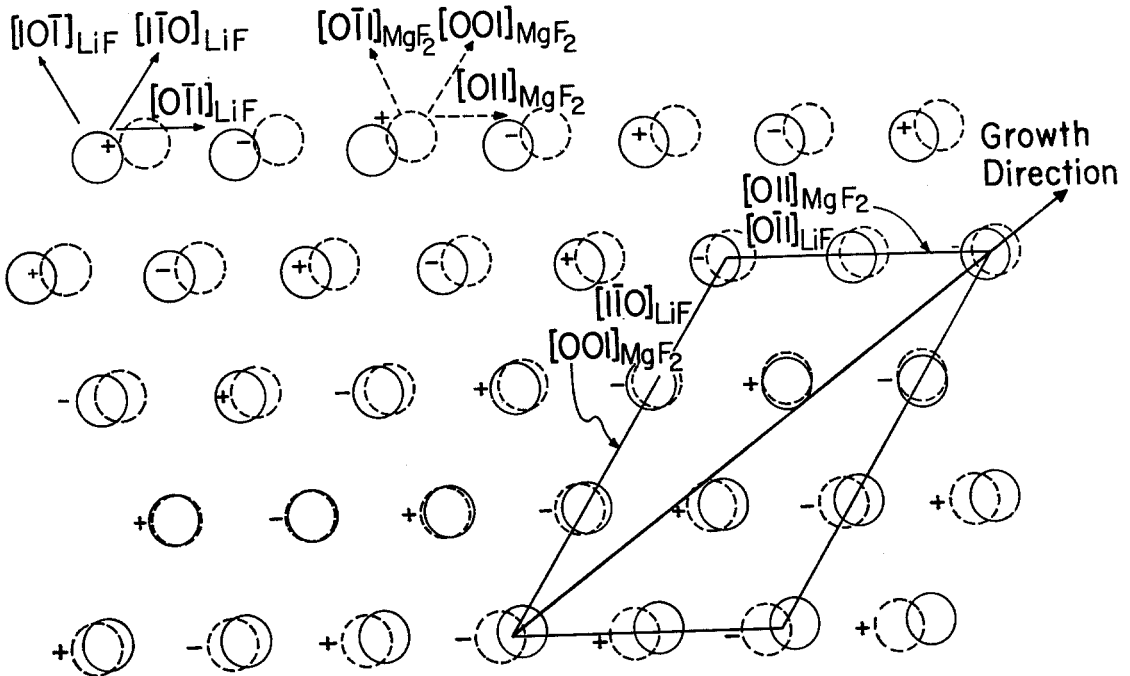


Figure 14 Hard-sphere model of the arrangement of atoms at the LiF/MgF₂ precipitate interface – superposition of (111)_{LiF} and (100)_{MgF₂} planes showing F⁻ ions in their equilibrium positions at the precipitate interface. Solid circles represent F⁻ ions in LiF and broken circles represent F⁻ ions in MgF₂. The + and – signs indicate that the F⁻ ions are slightly above or below the plane of drawing, which is (100)_{MgF₂}.

surprising, for Mg⁺⁺ and Cd⁺⁺ are usually considered to have the same ionic size as Li⁺ and Na⁺ respectively.

8.3. Kinetics

A Mg⁺⁺ ion will diffuse when it has a cation vacancy as a nearest neighbour and, therefore, it is only necessary to think of such associated pairs in the treatment of Mg⁺⁺ diffusion. The different states of association of Mg⁺⁺ ions with the extrinsic vacancies [16, 17] cause difficulty in knowing the concentration of associated pairs because the relative concentrations of the states change during precipitation. Generally, during precipitation reactions, there will be more associated pairs and higher order clusters than is indicated by the equilibrium data, simply owing to the fact that the solid solution is supersaturated. In view of these different states of the Mg⁺⁺ ions, let us now consider the kinetics of precipitate growth. If the growth of the particles is controlled by bulk diffusion of Mg⁺⁺, and if we assume that the concentration gradient in Fick's law is independent of temperature, then for the case where Mg⁺⁺ ions are highly associated with extrinsic vacancies, as

associated pairs [16], growth rate $\propto \exp(-\Delta H_m/kT)$, where ΔH_m is the activation energy for mobility of associated pairs.

In the kinetic measurements previously discussed, it is expected that the Mg⁺⁺ ions will be highly associated with vacancies, so that the above equation should be valid where growth is controlled by diffusion of associated pairs. In the case of the growth of metastable precipitates, good agreement is found between the activation energy for growth, 0.75 ± 0.25 eV, and the activation energy for diffusion of associated pairs which is of the order of 0.75 [18] to 0.79 eV [19]. These diffusion energies are obtained from measurements of dielectric loss, due to the rotation of associated pairs, as a function of time.

In marked contrast is the activation energy of 1.9 eV for growth of MgF₂ particles, and for the formation of MgF₂ from the metastable phase. One interpretation of these results is as follows. In the growth of the metastable phase, the precipitate is expected to have its crystal lattice continuous with that of the matrix apart from a few interface dislocations, so that growth should take place by Mg⁺⁺ ions jumping to, and across,

the interface. There would be no need for movement of the F⁻ ions. The MgF₂ particles, on the other hand, have a lattice quite distinct from that of the matrix and, except at the {111}_{LiF} habit plane, the atomic mismatch will be large. In the growth of MgF₂, it would then be necessary for a rearrangement of F⁻ ions as well as Mg⁺⁺ ions to take place at the precipitate interface (i.e. F⁻ ions must leave the LiF structure and jump across the boundary to gain the MgF₂ structure). Recent studies of anion diffusion in alkali halides [20-22] have shown the importance of cation/anion vacancy pairs. The concentration of these pairs is independent of the concentration of divalent impurities present. It is believed that the activation energy for diffusion of vacancy pairs would be equal to $E_s + E_m - E_b$, where E_s is the energy of formation of a Schottky defect, E_m is the energy of motion, and E_b is the binding energy of a vacancy pair. Substitution of reasonable values for E_s , E_m , and E_b would, however, give an activation energy for diffusion higher than 1.9 eV [20]. Experimental measurements on KCl doped with a divalent ion yield an activation energy for diffusion of 2.6 eV at high temperatures, but at low temperatures, where diffusion is structure-sensitive, values of 1.9 eV have been found [21]. Since LiF has similar values of E_s and E_m to KCl, and E_b should be similar for the two salts, it is expected that the activation energies for diffusion should be about the same in both cases. It therefore seems reasonable to propose a cation/anion vacancy pair mechanism for the growth of MgF₂ in LiF to account for the 1.9 eV activation energy determined experimentally.

8.4. Solubility

The solvus line determined in this study for precipitation of MgF₂ from LiF is shown in figs. 11 and 12 with data points from 0.045 to 6.5 mol % MgF₂ and is believed to be accurate to 1 or 2° C. This solvus line differs from that of Haven [7] by indicating greater solubility at all temperatures. It does, however, join up with the solvus line at higher concentrations, in the phase diagram shown in fig. 1. Haven used the lower knee of his ionic conductivity curves to determine his phase diagram, but this is not always clearly resolvable. He assumed the usual exponential expression for solubility:

$$C = A \exp(-E/2kT) \quad (2)$$

to extrapolate to high concentrations his results

at low concentrations (where C is the mole fraction of MgF₂ in solid solution, in equilibrium with the MgF₂ precipitates, at temperature T measured in degrees Kelvin). This procedure is inaccurate for alkali halide crystals doped with divalent ions because there is not a simple exponential relationship between the solute concentration and the reciprocal of the temperature [23].

The solvus line for the metastable phase, shown in fig. 11, is limited in range because the metastable phase transforms to MgF₂ at temperatures above 300° C. The 0.225 mol % MgF₂ datum point is therefore only approximate. The 0.045 mol % point, however, is quite accurate.

A theoretical analysis of solubility curves in monovalent/divalent halide systems to obtain enthalpies and entropies of solution has recently been presented [23]. The application of this analysis to the experimental curves given here will be published later.

In Haven's previous attempts to measure the solubility of CaCl₂, CdCl₂, and MnCl₂ in NaCl [24], it was assumed that the precipitating phase was the stable CaCl₂, CdCl₂·2NaCl, and MnCl, as indicated by the phase diagrams. It is virtually certain that these phases did not precipitate owing to difficulties in nucleation. Instead, it is expected that: (i) in the NaCl/CaCl₂ system, a metastable phase would form resembling the structure of CaCl₂ but matching up in two dimensions with the matrix as shown by Tolman [4]; (ii) in the NaCl/CdCl₂ system, the 6NaCl·CdCl₂ metastable phase would form as demonstrated by Suzuki [5]; (iii) in the NaCl/MnCl₂ system, some metastable phase, possibly like (i) or (ii), would form.

Allnatt and Jacobs [25] made the same kind of assumption as Haven in concluding that the lower temperature part of their ionic conductivity plot of KCl doped with SrCl₂ was due to the precipitation of SrCl₂. It is most probable that the precipitate is a metastable modification containing Sr⁺⁺ ions.

9. Relation to Other Alkali Halide Studies

Alkali halide crystals have been extensively studied for their ionic conductivity, dielectric loss, colour centre, and mechanical properties. Many of these studies have been based on the assumption that all of the divalent ions are in solid solution, even though the actual quantita-

tive knowledge of the solid solubility involved has been limited. Let us briefly consider the consequences of the observations of precipitation in the LiF/MgF₂ system on the following types of study.

9.1. Ionic Conductivity

Haven [7] first demonstrated with ionic conductivity the precipitation region in LiF doped with MgF₂. At his lowest MgF₂ concentrations, it is by no means certain which phase was precipitating. Since the MgF₂ and the metastable phase have distinctly different structures, they must give different ionic conductivity results in the precipitation region. A schematic ionic conductivity plot is shown in fig. 15 to

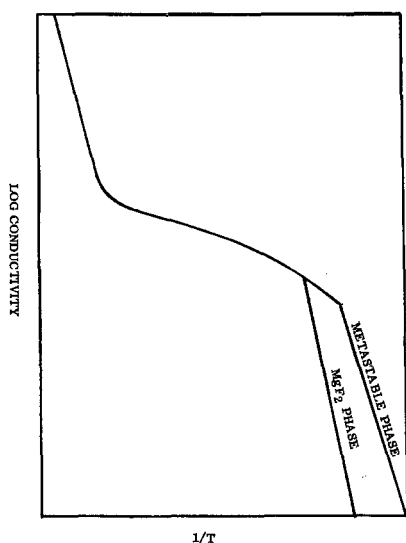


Figure 15 Schematic plot of ionic conductivity to show the type of result expected with different precipitate phases.

indicate the type of plot expected. This has in fact been observed [26] by taking ionic conductivity measurements on heating a LiF crystal which contained only the metastable precipitates, and then repeating the procedure with the same crystal containing only MgF₂ precipitates.

Without other means of detection of precipitation, it is often difficult to identify the start of precipitation from ionic conductivity plots. Bergé [27], for example, in studying MgF₂-doped LiF, has interpreted, as a region of association, a region of his ionic conductivity plot which extends to room temperature. However, the results of the present study

indicate that part of this region is caused by precipitation of the metastable phase. His interpretation of the ionic conductivity, including the low-temperature region, led Bergé to a binding energy of a Mg⁺⁺ ion/cation vacancy pair which is too high (i.e. 0.70 eV) compared with 0.36 [26] to 0.40 eV [28] from other studies.

9.2. Dielectric Loss

Measurements by Dryden [29-31] and co-workers, of dielectric loss in alkali halide crystals doped with divalent cations, have shown that, after quenching, the concentration of divalent ion/cation vacancy pairs decreases as a function of ageing-time. Their measurements were made on crystals containing concentrations of the order of 10⁻² mol % divalent cation, with ageing-temperatures generally below 100°C. Under these conditions, it seems likely, on the basis of our findings, that precipitation would occur. It is therefore concluded that the last stage of ageing in these dielectric loss experiments is due to the precipitation of divalent ions, probably as a metastable phase.

9.3. Colour Centres

Almost all studies of colour centres in doped alkali halide crystals neglect the state of the impurity ions prior to the colour centre experiment. Usually, crystals are heated to elevated temperatures to disperse the impurity ions and then are quickly cooled to room temperature. If the crystals are doped with concentrations of 10⁻² mol % impurity ions, or higher concentrations, it is quite possible that precipitation will occur by room-temperature ageing or by subsequent low-temperature heat-treatments.

A colour centre study has been made of LiF doped with MgF₂, with only a limited knowledge of precipitation in the system [32], which makes it difficult to understand fully the results. In another study of the same system, where precipitation is known to have occurred, it is not known whether the precipitate was MgF₂ or the metastable phase [33]. To be rigorous in these studies, it is necessary to know what fractions of the divalent ions exist in solid solution and as precipitate particles, and their respective effects on colour centre properties.

9.4. Mechanical Properties

Experimental studies [12, 34, 35] have been made of hardening of alkali halide crystals by

divalent ions, and theories [36-38] have been proposed to explain the results. In such studies as these, it is frequently assumed that the divalent ions are in solid solution. The present study, however, shows that precipitation usually occurs on slow cooling. It may even occur after rapid cooling followed by room-temperature ageing. It is therefore important in studies of mechanical properties to have a clear understanding of precipitation and to distinguish between solution-hardening and precipitation-hardening.

10. Summary and Conclusions

(a) In LiF doped with MgF₂, two types of precipitate can form depending on the rate of cooling and the composition. When heavily doped crystals (e.g. 2 mol % MgF₂) are slowly cooled, MgF₂ is precipitated. Rapid cooling of the same crystals, or even slow cooling of lightly doped crystals (e.g. 0.045 mol % MgF₂), causes the formation of a metastable phase.

(b) Precipitated MgF₂ particles are large, and are readily seen with the optical microscope to be blade-like with a saw-tooth-edge morphology. The MgF₂ particles appear to grow in a step-wise fashion, with each step probably having a $\{111\}_{\text{LiF}}$ habit plane and the resultant particle lying almost, but not exactly, parallel to a $\{111\}_{\text{LiF}}$ plane.

(c) There is an orientation relation between the LiF matrix and the MgF₂ precipitates of $\{111\}_{\text{LiF}} \parallel \{100\}_{\text{MgF}_2}$ and $[0\bar{1}1]_{\text{LiF}} \parallel [011]_{\text{MgF}_2}$ which gives a family of twenty-four different orientation combinations. A minority of the MgF₂ particles have an orientation with the same conjugate planes as given in the above definition, but with a range of directions in the $\{111\}_{\text{LiF}}$ plane between pairs of the six $[011]_{\text{MgF}_2}$ directions which lie at 7° apart.

(d) Metastable precipitates consist of intersecting $\{100\}$ platelets, which can only be seen in the electron microscope.

(e) The structure of the metastable phase is essentially the same as that proposed by Suzuki for the NaCl/CdCl₂ system (i.e. it has a cubic cell approximately double that of LiF in size, and presumably has a stoichiometry of 6LiF.MgF₂). Its cube axes are parallel to those of the LiF matrix.

(f) When crystals containing only the metastable precipitates are heated to about 300° C, MgF₂ nucleates at the metastable particles and grows at their expense.

(g) The nucleation rate of MgF₂ from solid solution is low, especially at low solute concentrations. It is possible that the MgF₂ always forms via the metastable phase.

(h) The metastable phase is always found to grow more rapidly than the MgF₂ phase. Kinetic measurements indicate activation energies 0.75 ± 0.25 and 1.9 ± 0.1 eV for the growth of the metastable phase and the MgF₂ respectively. It is believed that the growth of the metastable phase is controlled by diffusion of Mg⁺⁺ ion/cation vacancy pairs through the LiF matrix, whereas the growth of MgF₂ is controlled by vacancy pair motion, probably at the precipitate/matrix interface.

(i) Solubility measurements indicate that, at low concentrations of MgF₂, the solvus line for MgF₂ precipitation, proposed by Haven [7], is inaccurate and that it gives values of solubility which are too low. At higher concentrations of MgF₂, the present solubility results agree with the phase diagram determined by Counts, Roy, and Osborn [8].

(j) A solvus line for the precipitation of the metastable phase has been established at concentrations up to 0.225 mol % MgF₂.

(k) Precipitation of the metastable phase can readily occur even at low concentrations and it must therefore be seriously considered in measurements of ionic conductivity, dielectric loss, mechanical properties, and in colour centre experiments, done at temperatures below about 300° C.

Acknowledgements

We would like to acknowledge the assistance of the following people, employed by the Cornell Materials Science Center: Mr G. Shen, for work on the electron microscope; Miss M. Rich, for X-ray diffraction work; Mrs C. Newton, for photographic work; Professor Pohl's crystal-growing group, for crystals grown by the Czochralski technique; and Arne Berger, for general help in the summer of 1965. In addition, Dr R. W. Hendricks provided stimulating discussions and criticisms.

This research was carried out at Cornell University and was financially supported by the Advanced Research Projects Agency, through the Cornell Materials Science Center, and by the National Science Foundation.

References

1. S. MIYAKE and K. SUZUKI, *J. Phys. Soc. Japan* **9** (1954) 702.

2. K. SUZUKI, *ibid* **10** (1955) 794.
3. *Idem*, *ibid* **13** (1958) 179.
4. K. TOLMAN, *Czech. J. Phys.* **13** (1963) 296.
5. K. SUZUKI, *J. Phys. Soc. Japan* **16** (1961) 67.
6. K. TOLMAN, *Czech. J. Phys.* **12** (1962) 542.
7. Y. HAVEN, *Rec. Trav. Chim. Pay-Bas* **69** (1950) 1471, 1505.
8. W. E. COUNTS, R. ROY, and E. F. OSBORN, *J. Ceram. Soc.* **36** (1953) 12.
9. E. LILLEY and J. B. NEWKIRK, "Advances in X-ray Analysis", Vol. 7, edited by W. M. Mueller, G. R. Mallett, and M. J. Fay (Plenum Press, New York, 1964).
10. J. WASHBURN and J. NADEAU, *Acta Met.* **6** (1958) 665.
11. B. D. CULLITY, "Elements of X-ray Diffraction" (Addison Wesley, New York, 1956).
12. W. G. JOHNSTON, *J. Appl. Phys.* **33** (1962) 2050.
13. A. C. DAMASK and G. J. DIENES, "Point Defects in Metals" (Gordon and Breach, New York, 1963).
14. J. H. HOLLOMAN and D. TURNBULL, *Progress in Metal Physics* **4** (1953) 33.
15. R. G. WYCKOFF, "Crystal Structures", Vols. I and II (Wiley, New York, 1963 and 1964).
16. A. B. LIDIARD, "Handbuch der Physik", Vol. 20, edited by S. Flugge (Springer-Verlag, Berlin, 1957), p. 246.
17. *Idem*, *J. Appl. Phys.* **33** (1962) 414.
18. J. PETIAU, *J. de Physique* **24** (1963) 564.
19. J. S. DRYDEN, S. MORIMOTO, and J. S. COOK, *Phil. Mag.* **10** (1965) p. 320.
20. N. LAURENCE, *Phys. Rev.* **120** (1960) 57.
21. L. W. BARR, I. M. HOODLESS, J. A. MORRISON, and R. RUDHAM, *Trans. Faraday Soc.* **56** (1960) 697.
22. R. G. FULLER, *Phys. Rev.* **142** (1966) 542.
23. E. LILLEY, Ph.D. thesis, Cornell University (1966).
24. Y. HAVEN, Report of the Conference on Defects in Crystalline Solids, The Physical Society, London (1954), p. 261.
25. A. R. ALLNATT and P. W. M. JACOBS, *Trans. Faraday Soc.* **58** (1962) 116.
26. E. BARSIS, E. LILLEY, and A. TAYLOR, *Proc. Brit. Ceram. Soc.* (to be published).
27. P. BERGÉ, *Bull. Soc. Franc. Miner. Crist.* **83** (1960) 57.
28. T. STOEBE and P. L. PRATT, *Proc. Brit. Ceram. Soc.* (to be published).
29. J. S. COOK and J. S. DRYDEN, *Austral. J. Phys.* **13** (1960) 260.
30. *Idem*, *Proc. Phys. Soc. (London)* **80** (1962) 479.
31. J. S. DRYDEN, Paper II C-6, Conference on Crystal Lattice Defects, Kyoto (1962), *J. Phys. Soc. Japan* **18** Suppl. III (1963) 129.
32. P. DUBOIS, P. BERGÉ, M. BENVENISTE, and G. BLANC, *J. de Phys.* **25** (1964) 1017.
33. J. MORT, *Solid State Comm.* **3** (1965) 263.
34. R. P. HARRISON, P. L. PRATT, and C. W. A. NEWEY, *Proc. Brit. Ceram. Soc.* **1** (1964) 197.
35. C. W. A. NEWEY, *Trans. Brit. Ceram. Soc.* **62** (1963) 739.
36. R. FLEISCHER, *Acta Met.* **10** (1962) 835.
37. *Idem*, *J. Appl. Phys.* **33** (1962) 3504.
38. R. CHANG and L. J. GRAHAM, *Acta Cryst.* **17** (1964) 795.